Monthly Notices
of the
ROYAL ASTRONOMICAL SOCIETY

MNRAS **476,** L1–L5 (2018)
Advance Access publication 2018 February 6

doi:10.1093/mnrasl/sly019

Where the Solar system meets the solar neighbourhood: patterns in the distribution of radiants of observed hyperbolic minor bodies

Carlos de la Fuente Marcos,[1]★ Raúl de la Fuente Marcos[1] and Sverre J. Aarseth[2]

[1] *Universidad Complutense de Madrid, Ciudad Universitaria, E-28040 Madrid, Spain*
[2] *Institute of Astronomy, University of Cambridge, Madingley Road, Cambridge CB3 0HA, UK*

Accepted 2018 February 1. Received 2018 January 31; in original form 2017 December 1

ABSTRACT

Observed hyperbolic minor bodies might have an interstellar origin, but they can be natives of the Solar system as well. Fly-bys with the known planets or the Sun may result in the hyperbolic ejection of an originally bound minor body; in addition, members of the Oort cloud could be forced to follow inbound hyperbolic paths as a result of secular perturbations induced by the Galactic disc or, less frequently, due to impulsive interactions with passing stars. These four processes must leave distinctive signatures in the distribution of radiants of observed hyperbolic objects, both in terms of coordinates and velocity. Here, we perform a systematic numerical exploration of the past orbital evolution of known hyperbolic minor bodies using a full *N*-body approach and statistical analyses to study their radiants. Our results confirm the theoretical expectations that strong anisotropies are present in the data. We also identify a statistically significant overdensity of high-speed radiants towards the constellation of Gemini that could be due to the closest and most recent known fly-by of a star to the Solar system, that of the so-called Scholz's star. In addition to and besides 1I/2017 U1 ('Oumuamua), we single out eight candidate interstellar comets based on their radiants' velocities.

Key words: methods: statistical – celestial mechanics – comets: general – minor planets, asteroids: general – Oort Cloud – solar neighbourhood.

1 INTRODUCTION

The discovery (Bacci et al. 2017; Meech et al. 2017a) and the subsequent study (see e.g. Bannister et al. 2017; Jewitt et al. 2017; Knight et al. 2017; Masiero 2017; Meech et al. 2017b; Ye et al. 2017; Bolin et al. 2018; Fitzsimmons et al. 2018) of the first bona fide interstellar minor body, 1I/2017 U1 ('Oumuamua), has brought the subject of hyperbolic minor bodies into the spotlight. Although some of the known ones might have had an interstellar origin like 'Oumuamua, others (perhaps most of them) could be natives of the Solar system. There are mechanisms capable of generating hyperbolic objects other than interstellar interlopers. They include close encounters with the known planets or the Sun, for objects already traversing the Solar system inside the trans-Neptunian belt; but also secular perturbations induced by the Galactic disc or impulsive interactions with passing stars, for more distant bodies (see e.g. Fouchard et al. 2011, 2017; Królikowska & Dybczyński 2017). These last two processes have their sources beyond the Solar system and may routinely affect members of the Oort cloud (Oort 1950), driving them into inbound hyperbolic paths that may cross the inner Solar system, making them detectable from the Earth (see e.g. Stern 1987).

Each and every object approaching from the outskirts of the Solar system appears to come from its own well-defined, unique location in the sky, its radiant or antapex, and has a characteristic barycentric velocity that carries valuable information about its provenance. The four processes listed above can induce strong anisotropies and leave distinctive signatures in the observed distribution of radiants, both in terms of coordinates and velocity. The impact of some of these mechanisms on the perihelia of long-period comets has been well studied (see e.g. Matese & Whitmire 1996; Matese, Whitman & Whitmire 1997; Dybczyński 2002; Horner & Evans 2002), but the properties of the radiants of observed hyperbolic (eccentricity >1) minor bodies have never been studied in detail. Here, we carry out a systematic numerical exploration of the past orbital evolution of known hyperbolic objects using a full *N*-body approach and statistical analyses to study their radiants. This Letter is organized as follows. Section 2 introduces the tools used and the input data. The distribution of radiants is presented and discussed in Section 3. The sample of internally produced hyperbolic minor bodies is examined in Section 4. In Section 5, we study the population of former members of the Oort cloud. Candidate interstellar interlopers are singled out in Section 6. Results are discussed and conclusions are summarized in Section 7.

2 TOOLS AND INPUT DATA

For minor bodies with very long orbital periods and extremely elongated orbits, the properties of their perihelia/aphelia encode a

★ E-mail: nbplanet@ucm.es

significant amount of interesting dynamical information (see e.g. Horner & Evans 2002); for those currently following hyperbolic paths, an equally relevant source of knowledge is in the radiant or point in the sky from which the incoming object appears to originate. The analysis of the properties of the radiants of these interesting bodies can help in understanding their origin and evolution. Aiming at extracting useful information – namely, the positional and velocity distributions – we have computed the properties of the radiants associated with the orbit determinations available for these objects using full N-body simulations carried out with a code written by Aarseth (2003)[1] that implements a fourth-order version of the Hermite scheme described by Makino (1991) without including any non-gravitational forces. The model Solar system used in our calculations includes the perturbations from the eight major planets, with the Earth–Moon system as two separate bodies. In addition, it incorporates the barycenter of the dwarf planet Pluto–Charon system and the three most massive asteroids of the main belt. Positions and velocities in the barycentre of the Solar system for these bodies at epoch JD 2458000.5 (2017-September-04.0 TDB, Barycentric Dynamical Time) have been provided by Jet Propulsion Laboratory's (JPL) HORIZONS;[2] additional details are given in de la Fuente Marcos & de la Fuente Marcos (2012). Here, the present-day orbits of the known hyperbolic minor bodies – 339 with nominal heliocentric eccentricity >1, data as of 2018 January 18 – are integrated backwards for 0.1 Myr to compute the properties of their associated radiants. For these calculations, we use input data provided by JPL's Solar System Dynamics Group Small-Body Database (SSDG SBDB; Giorgini 2015)[3] and the Minor Planets Center (MPC) Database (Rudenko 2016).[4] As a reference and for a minor body moving with an inbound velocity of 1 km s^{-1} – i.e. it may travel 10 000 au in less than 50 000 yr – that is the value of the escape velocity at about 2 000 au, our 0.1 Myr integrations back in time place such an object beyond 20 000 au from the Sun, i.e. at the outer Oort cloud (see e.g. Hills 1981).

3 THE DISTRIBUTION OF RADIANTS

The histograms presented in this section use a bin width computed using the Freedman–Diaconis rule (Freedman & Diaconis 1981), i.e. 2 IQR $n^{-1/3}$, where IQR is the interquartile range and n is the number of data points. Averages, standard deviations, medians, IQRs, and other statistical parameters have been computed in the usual way (see e.g. Wall & Jenkins 2012); we adopt Poisson statistics ($\sigma = \sqrt{n}$) to compute the error bars – applying the approximation given by Gehrels (1986) when $n < 21$, $\sigma \sim 1 + \sqrt{0.75 + n}$.

Fig. 1 shows the distribution of geocentric equatorial coordinates of the radiants of known hyperbolic minor bodies computed using the input data and the procedure described in the previous section. Here, the bin widths are $3^{\rm h}.69$ (top panel) and $16^{\circ}.57$ (bottom panel). The distribution in right ascension, α, is somewhat asymmetric (top panel) with 193 radiants (out of 339) in the interval ($0^{\rm h}$, $12^{\rm h}$). This is a 2.55σ departure from an isotropic distribution, where $\sigma = \sqrt{n}/2$ is the standard deviation for binomial statistics (see e.g. Wall & Jenkins 2012). The presence of this asymmetry might not be the result of observational bias because the radiant is not directly observed but computed once the orbit determination is obtained. On the other hand, such asymmetry could be consistent with the one induced by a stellar passage through the Oort cloud (see e.g. Dybczyński 2002). The distribution in declination, δ, is asymmetric as well (bottom panel), but evenly distributed in terms of hemispheres as 176 radiants have southern declinations.

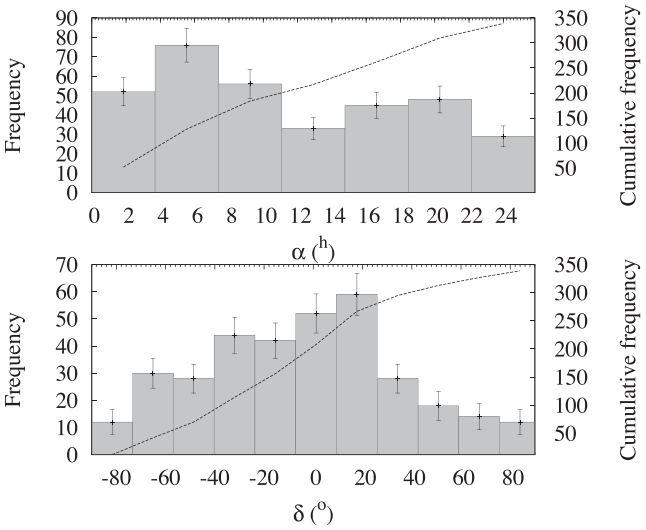

Figure 1. Distribution of the geocentric equatorial coordinates of the radiants of known hyperbolic minor bodies (nominal orbits); cumulative frequency in dashes, error bars from Poisson statistics (see Section 3).

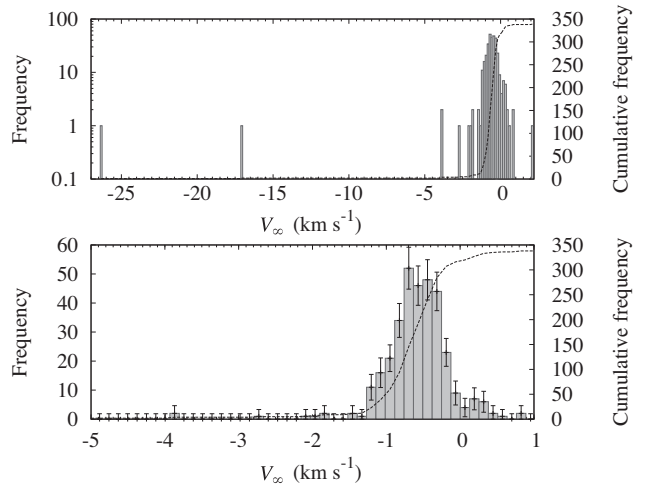

Figure 2. Distribution of the radiants' velocities of known hyperbolic minor bodies (cumulative frequency in dashes). The bottom panel magnifies the section of the top one that includes most of the data.

Fig. 2 shows the radiant's velocity, V_∞ (actually its proxy, the velocity at the end of the calculations), histogram of the sample in Fig. 1; the bottom panel focuses on the bins with most of the entries, the bin width is 0.13 km s^{-1}. The distribution is not Gaussian – i.e. the average and standard deviation, -0.7 ± 1.7 km s^{-1}, cannot be used to describe the velocity distribution adequately – and includes a number of outliers (see Section 6). Out of 339 objects, 316 or 93.2 per cent shows inbound (i.e. negative) barycentric velocities. The non-Gaussianity of the distribution suggests that multiple processes may be shaping the observed velocity spread.

Fig. 3 shows the distribution in equatorial coordinates of the radiants in Fig. 1. The distribution exhibits a number of distinct concentrations that lead to the asymmetries present in Fig. 1. These

[1] http://www.ast.cam.ac.uk/~sverre/web/pages/nbody.htm
[2] https://ssd.jpl.nasa.gov/?horizons
[3] https://ssd.jpl.nasa.gov/sbdb.cgi
[4] https://minorplanetcenter.net/db_search

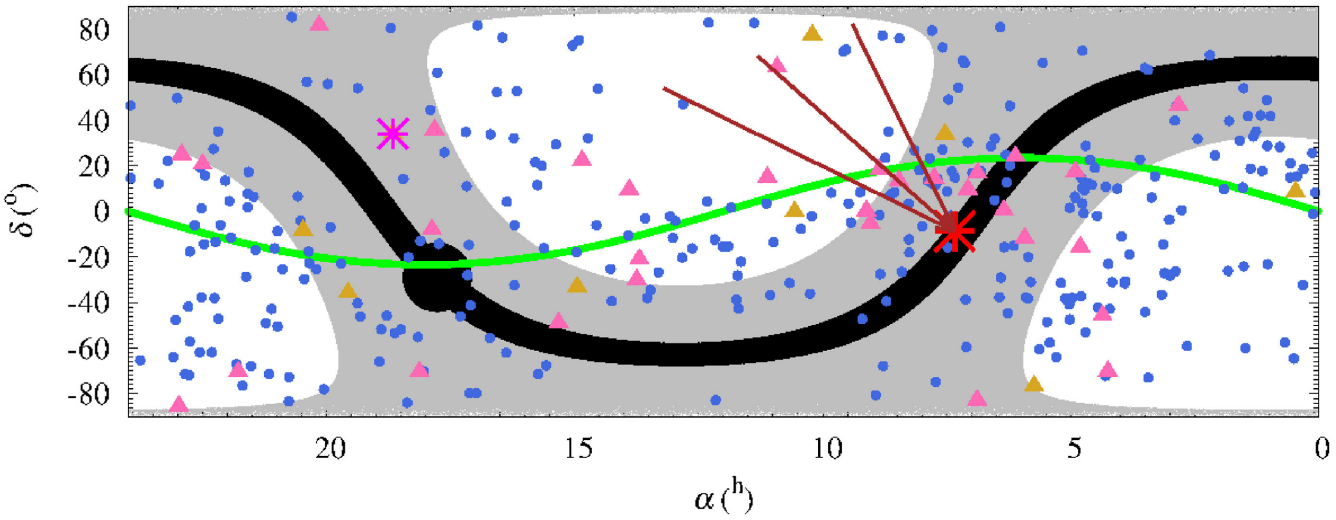

Figure 3. Distribution of radiants of known hyperbolic minor bodies in the sky. The radiant of 1I/2017 U1 ('Oumuamua) is represented by a pink star, those objects with radiant's velocity > -1 km s^{-1} are plotted as blue filled circles, the ones in the interval $(-1.5, -1.0)$ km s^{-1} are shown as pink triangles, and those < -1.5 km s^{-1} appear as goldenrod triangles. The current position of the binary star WISE J072003.20-084651.2, also known as Scholz's star, is represented by a red star, the convergent brown arrows represent its motion and uncertainty as computed by Mamajek et al. (2015). The ecliptic is plotted in green. The Galactic disc, which is arbitrarily defined as the region confined between Galactic latitude $-5°$ and $5°$, is outlined in black, the position of the Galactic Centre is represented by a filled black circle; the region enclosed between Galactic latitude $-30°$ and $30°$ appears in grey. Data source: JPL's SSDG SBDB.

clusters of radiants are well away from that of 1I/2017 U1 ('Oumuamua), the pink star in Fig. 3. The most obvious overdensity – at $\alpha = 7\overset{h}{.}4$ and $\delta = +16\overset{\circ}{.}6$ – may have as many as 36 radiants, or nearly 11 per cent of all the known ones, and about 22 per cent (9/41) of the ones with radiant's velocity < -1 km s^{-1}. Relevant comets in this group are C/1999 S4 (LINEAR), C/2007 W1 (Boattini), C/2010 X1 (Elenin), C/2012 S1 (ISON), or C/2013 A1 (Siding); some of them have experienced fragmentation/disintegration events near perihelion. Other clusterings are observed towards $\alpha = 4\overset{h}{.}6$ and $\delta = +10\overset{\circ}{.}0$ – 14 possible members, relevant comets are C/1956 F1-A (Wirtanen), C/1999 N4 (LINEAR), or C/2017 M4 (ATLAS) – and $\alpha = 5\overset{h}{.}5$ and $\delta = -39\overset{\circ}{.}0$ – 16 possible members, relevant comets are C/1890 F1 (Brooks), C/2009 K5 (McNaught), or C/2013 G3 (PANSTARRS). Clusterings are also found in the distribution of poles and perihelia of hyperbolic minor bodies (de la Fuente Marcos & de la Fuente Marcos 2017), but these can be due to observational bias (particularly, the perihelion positions).

The distribution of radiants in Fig. 3 shows a number of conspicuous concentrations or overdensities both for the full sample and for the subsample of objects with velocity < -1 km s^{-1} (plotted in pink and goldenrod); however, it is unclear from the figure whether any of these overdensities are statistically significant. In order to make an informed decision, we have used a population of hypothetical isotropic detections of the same size as reference. Such data set has been obtained by generating points uniformly distributed on the surface of the celestial sphere using an algorithm due to Marsaglia (1972). The positions of these points in the sky have $\alpha \in (0^h, 24^h)$ and $\delta \in (-90°, 90°)$. The excess of observed radiants with respect to a uniformly distributed sample has been quantified by generating random points to cover the surface of the celestial sphere and counting how many real and random radiants are found within $10°$ (our counting radius) of each random point. Our statistics is the difference between real and uniformly distributed counts; as we are studying excesses not voids, negative differences are customarily assigned a value of zero. Our experiments consider 2×10^5 random points (and counts) to scan the celestial sphere; multiple random

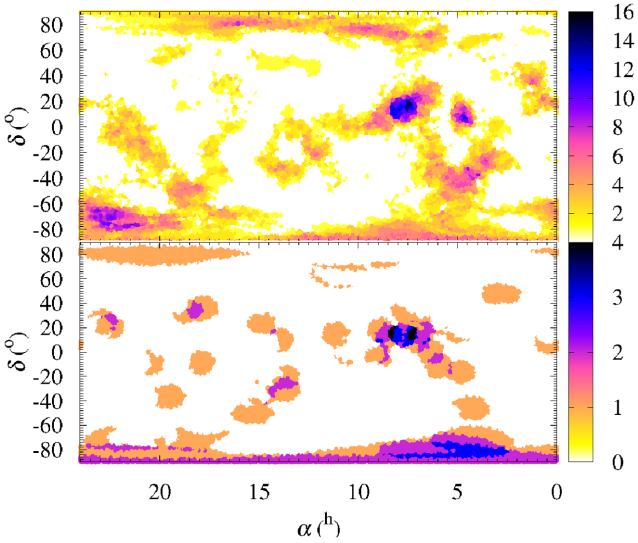

Figure 4. Statistical significance analysis of the distribution of radiants in Fig. 3. Difference between counts from a scan of the observed sample and that of an isotropic one; full sample analysis (top panel) and that of the subsample with velocity < -1 km s^{-1} (bottom panel).

samples and several radii ($5°$ and $15°$) were tested to confirm that our overall results were neither affected by our choice of counting radius nor by the actual random sample. Our analysis has been performed on the full sample – Fig. 4, top panel, average difference of 1.3 ± 1.9, median of 0, IQR = 2 – and the subsample with velocity < -1 km s^{-1} – Fig. 4, bottom panel, average difference of 0.3 ± 0.6, median of 0, IQR = 0. Fig. 4 confirms that the overall spatial distribution of radiants of observed hyperbolic minor bodies is far from uniform and strongly anisotropic with several statistically significant overdensities (up to 7.7σ) present in the data. The most relevant cluster of radiants is present in both panels and it is located towards Gemini (see Section 5 for a detailed analysis). Other significant

concentrations are observed towards $\alpha \sim 5^{\rm h}$, $\delta \sim +10^\circ$ (top panel) and also $\alpha = 3\overset{\rm h}{.}3 \pm 0\overset{\rm h}{.}3$, $\delta = -79\overset{\circ}{.}3 \pm 0\overset{\circ}{.}4$ (bottom panel).

4 INDIGENOUSLY PRODUCED HYPERBOLICS

Fig. 2 shows a tail of currently hyperbolic comets that, when integrated backwards, do not show inbound, i.e. negative, velocities but outbound ones. In fact, our simulations show that these objects (about 10 per cent of the entire sample) were following elliptical paths in the past, i.e. were bound to the Solar system, but they were ejected after experiencing close encounters with the known planets and/or the Sun. Some comets that may have become hyperbolic in recent times could be C/1994 N1 (Nakamura-Nishimura-Machholz) or C/2003 T4 (LINEAR). This might also be the case of comet C/1980 E1 (Bowell), which has a spectrum consistent with an origin in the Solar system (Jewitt et al. 1982) and now has the second largest value of the eccentricity, $e = 1.0577$ ($\sim 11\,500\sigma$), after that of 1I/2017 U1 ('Oumuamua), $e = 1.1995$ ($\sim 1100\sigma$). Such a high eccentricity might have been acquired after a fly-by with Jupiter (Buffoni, Scardia & Manara 1982; Branham 2013). Former interstellar comets, like 96P/Machholz 1 (Langland-Shula & Smith 2007; Schleicher 2008), might also be eventually returned to deep space (de la Fuente Marcos, de la Fuente Marcos & Aarseth 2015). The Solar system is also the source of some artificially produced hyperbolic objects. Five spacecraft – Pioneer 10 and 11, Voyager 1 and 2, and New Horizons – currently have outbound hyperbolic velocities with respect to the barycentre of the Solar system in excess of $10\,{\rm km\,s^{-1}}$ that will lead them to deep space (McNutt & Zurbuchen 2016).

5 OORT CLOUD SOURCES

The bulk of the distribution in Fig. 2 is probably compatible with the so-called Oort spike of new comets (see e.g. Fouchard et al. 2017; Królikowska & Dybczyński 2017); in addition, the clusterings visible in Figs 3 and 4 could be consistent with some sort of weak comet shower coming from those directions (see e.g. Dybczyński 2002; Fouchard et al. 2017). Figs 3 and 4 show a statistically significant overdensity of hyperbolic comets with radiant inbound velocities $>1\,{\rm km\,s^{-1}}$ located towards the coordinates $\alpha = 7^{\rm h}25^{\rm m}23^{\rm s}$ and $\delta = +16^\circ 38' 43''$ ($111\overset{\circ}{.}3 \pm 0\overset{\circ}{.}7$, $+16\overset{\circ}{.}6 \pm 1\overset{\circ}{.}1$) in the constellation of Gemini. This location is well away from both Solar apex and antapex. Most comets with radiants within the overdensity are widely regarded as new or Oort cloud comets. The presence of a coherent set of radiants hints at the outcome of a relatively recent stellar fly-by. Although the research on past and future close encounters between passing stars and the Solar system is still affected by significant uncertainties (see e.g. Bailer-Jones 2015, 2018; Dybczyński & Berski 2015), there is one case in which the dynamical parameters of the fly-by are relatively well determined, that of the so-called Scholz's star (Mamajek et al. 2015) – HIP 14473, other recent stellar fly-by, may have approached within 0.22 pc, but 3.78 Myr ago (Dybczyński & Berski 2015; Feng & Bailer-Jones 2015). The current position of the binary star WISE J072003.20-084651.2 (Scholz 2014; Burgasser et al. 2015) is plotted in Fig. 3 as a red star, the convergent brown arrows represent its motion and uncertainty as computed by Mamajek et al. (2015). This low-mass binary may have passed 52^{+23}_{-14} kau from the Sun, 70^{+15}_{-10} kyr ago; at its closest approach, it may have moved projected towards $\alpha = 11\overset{\rm h}{.}3 \pm 1\overset{\rm h}{.}9$ and $\delta = +68^\circ \pm 14^\circ$ (this area in Fig. 3 shows a relative void in the distribution of radiants). It is difficult to attribute to mere chance the near coincidence in terms of timing and position in the sky between the most recent known stellar fly-by and the statistically significant overdensity visible in Figs 3 and 4. It is unclear whether other clusterings present may have the same origin or be the result of other, not-yet-documented, stellar fly-bys or perhaps interactions with one or more unseen perturbers orbiting the Sun well beyond Neptune (see e.g. de la Fuente Marcos & de la Fuente Marcos 2014; Trujillo & Sheppard 2014; Batygin & Brown 2016).

6 INTERSTELLAR INTERLOPERS

Fig. 2 shows a tail of hyperbolic minor bodies with inbound velocities well in excess of the median value of the radiant's velocity, $-0.57\,{\rm km\,s^{-1}}$. In order to select candidates that may have an interstellar origin, we adopt the cut-off value of $-1.5\,{\rm km\,s^{-1}}$; the difference between this value and the median is over twice the IQR, $0.44\,{\rm km\,s^{-1}}$, in absolute terms. Given the distribution in Fig. 2, we believe that any object with an inbound velocity $<-1.5\,{\rm km\,s^{-1}}$ is a reasonably good candidate to be an interstellar interloper – the lower fence of Tukey's method (Tukey 1977) to identify statistical outliers is $Q_1 - 1.5\ {\rm IQR} = -1.45\,{\rm km\,s^{-1}}$, where Q_1 is the lower quartile. Apart from 1I/2017 U1 ('Oumuamua), our list includes C/1853 R1 (Bruhns), C/1997 P2 (Spacewatch), C/1999 U2 (SOHO), C/2002 A3 (LINEAR), C/2008 J4 (McNaught), C/2012 C2 (Bruenjes), C/2012 S1 (ISON), and C/2017 D3 (ATLAS). Each candidate's radiant tends to be relatively well separated from the others (see Fig. 3), which suggests that they are dynamically uncorrelated. The best candidates are however C/2008 J4 (McNaught) and C/2012 S1 (ISON) as their orbit determinations are more reliable than those of the others. In both cases, the inbound velocity is close to $4\,{\rm km\,s^{-1}}$ that is well away from that of the bulk of objects in Fig. 2, bottom panel. Although C/1999 U2 might have had $V_\infty = -17.1\,{\rm km\,s^{-1}}$, the object might not be currently hyperbolic – may now be captured as C/2005 W5 (Kracht et al. 2005) – but it was probably hyperbolic in the past. Interstellar interlopers could be the result of the gravitational slingshot effect – first discussed within the context of dense stellar systems by Saslaw, Valtonen & Aarseth (1974). The prospect of detecting these bodies has been considered for decades (see e.g. Cook et al. 2016; Engelhardt et al. 2017; Trilling et al. 2017).

7 DISCUSSION AND CONCLUSIONS

In sharp contrast to their bound counterparts and due to their unique nature, the orbital solutions of hyperbolic minor bodies are based on relatively brief arcs of observation and this fact has an impact on their reliability. Our results depend on the quality of the available orbit determinations, over 60 per cent of the solutions used here have uncertainties comparable or better than those associated with that of 1I/2017 U1 ('Oumuamua) – errors in α, δ, and V_∞ are less than or close to $0\overset{\rm h}{.}01$, $0\overset{\circ}{.}05$, and $0.1\,{\rm km\,s^{-1}}$, respectively. This also applies to those objects being part of the overdensities of radiants identified here. Out of 339 objects in the sample, 232 have reported uncertainties and 212 have eccentricity with statistical significance above 3σ – i.e. $(e-1)/\sigma > 3$. Therefore, the overall conclusions of our investigation are expected to be essentially correct, but those of some individual objects might not be. Regarding the statistical significance of the overdensities present in Fig. 4, the application of Tukey's method gives an upper fence value – $Q_3 + 1.5$ IQR, where Q_3 is the upper quartile – for outliers of 5 for the top panel and 0 for the bottom panel, i.e. the overdensities are indeed statistically significant according to Tukey's criterion.

In this Letter, we have explored the distribution of the radiants of observed hyperbolic minor bodies, both in terms of location in the sky and kinematics. Our *N*-body calculations and subsequent statistical analyses lead to the following conclusions:

(i) The distribution of the radiants of observed hyperbolic minor bodies is strongly anisotropic.

(ii) Consistent with theoretical expectations, the distribution of radiants' velocities may result from the concurrent action of four dynamical processes: local planetary (and Solar) fly-bys, external secular, and impulsive perturbations on the Oort cloud, and crossing paths with interstellar interlopers.

(iii) A statistically significant overdensity of hyperbolic comets with radiant's inbound velocity $>1\,\mathrm{km\,s^{-1}}$ appears located towards the coordinates $\alpha = 7^{\mathrm{h}}25^{\mathrm{m}}23^{\mathrm{s}}$, $\delta = +16^{\circ}38'43''$ ($111\overset{\circ}{.}3 \pm 0\overset{\circ}{.}7$, $+16\overset{\circ}{.}6 \pm 1\overset{\circ}{.}1$) in the constellation of Gemini.

(iv) The overdensity of high-speed radiants appears to be consistent in terms of location and time constraints with the latest known stellar fly-by, that of Scholz's star.

(v) Based on their current orbit determinations, eight hyperbolic comets emerge as good candidates to have an interstellar origin as they all have $V_\infty < -1.5\,\mathrm{km\,s^{-1}}$: C/1853 R1 (Bruhns), C/1997 P2 (Spacewatch), C/1999 U2 (SOHO), C/2002 A3 (LINEAR), C/2008 J4 (McNaught), C/2012 C2 (Bruenjes), C/2012 S1 (ISON), and C/2017 D3 (ATLAS).

ACKNOWLEDGEMENTS

We thank the anonymous referee for helpful comments and suggestions. CdlFM and RdlFM thank A. I. Gómez de Castro of the Universidad Complutense de Madrid (UCM) for providing access to computing facilities. This work was partially supported by the Spanish 'Ministerio de Economía y Competitividad' (MINECO) under grant ESP2014-54243-R. Part of the calculations and the data analysis were completed on the EOLO cluster of the UCM, and we thank S. Cano Alsúa for his help during this stage. EOLO, the HPC of Climate Change of the International Campus of Excellence of Moncloa, is funded by the MECD and MICINN. In preparation of this Letter, we made use of the NASA Astrophysics Data System, the ASTRO-PH e-print server, and the MPC data server.

REFERENCES

Aarseth S. J., 2003, Gravitational *N*-body simulations. Cambridge Univ. Press, Cambridge, p. 27
Bacci P. et al., 2017, MPEC Circ., MPEC 2017-U181
Bailer-Jones C. A. L., 2015, A&A, 575, A35
Bailer-Jones C. A. L., 2018, A&A, 609, A8
Bannister M. T. et al., 2017, ApJ, 851, L38
Batygin K., Brown M. E., 2016, AJ, 151, 22
Bolin B. T. et al., 2018, ApJ, 852, L2
Branham R. L., Jr, 2013, RMxAA, 49, 111
Buffoni L., Scardia M., Manara A., 1982, M&P, 26, 311
Burgasser A. J. et al., 2015, AJ, 149, 104
Cook N. V., Ragozzine D., Granvik M., Stephens D. C., 2016, ApJ, 825, 51
de la Fuente Marcos C., de la Fuente Marcos R., 2012, MNRAS, 427, 728
de la Fuente Marcos C., de la Fuente Marcos R., 2014, MNRAS, 443, L59
de la Fuente Marcos C., de la Fuente Marcos R., 2017, Res. Notes AAS, 1, 5
de la Fuente Marcos C., de la Fuente Marcos R., Aarseth S. J., 2015, MNRAS, 446, 1867
Dybczyński P. A., 2002, A&A, 396, 283
Dybczyński P. A., Berski F., 2015, MNRAS, 449, 2459
Engelhardt T., Jedicke R., Vereš P., Fitzsimmons A., Denneau L., Beshore E., Meinke B., 2017, AJ, 153, 133
Feng F., Bailer-Jones C. A. L., 2015, MNRAS, 454, 3267
Fitzsimmons A et al., 2018, Nature Astron., 2, 133
Fouchard M., Rickman H., Froeschlé C., Valsecchi G. B., 2011, A&A, 535, A86
Fouchard M., Rickman H., Froeschlé C., Valsecchi G. B., 2017, A&A, 604, A24
Freedman D., Diaconis P., 1981, Z. Wahrscheinlichkeitstheor. Verwandte Geb., 57, 453
Gehrels N., 1986, ApJ, 303, 336
Giorgini J. D., 2015, IAU General Assembly, Meeting #29, 22, 2256293
Hills J. G., 1981, AJ, 86, 1730
Horner J., Evans N. W., 2002, MNRAS, 335, 641
Jewitt D. C., Soifer B. T., Neugebauer G., Matthews K., Danielson G. E., 1982, AJ, 87, 1854
Jewitt D., Luu J., Rajagopal J., Kotulla R., Ridgway S., Liu W., Augusteijn T., 2017, ApJ, 850, L36
Knight M. M., Protopapa S., Kelley M. S. P., Farnham T. L., Bauer J. M., Bodewits D., Feaga L. M., Sunshine J. M., 2017, ApJ, 851, L31
Kracht R., Hammer D., Marsden B. G., Sekanina Z., Chodas P., 2005, MPEC Circ., MPEC 2005-Y27
Królikowska M., Dybczyński P. A., 2017, MNRAS, 472, 4634
Langland-Shula L. E., Smith G. H., 2007, ApJ, 664, L119
Makino J., 1991, ApJ, 369, 200
Mamajek E. E., Barenfeld S. A., Ivanov V. D., Kniazev A. Y., Väisänen P., Beletsky Y., Boffin H. M. J., 2015, ApJ, 800, L17
Marsaglia G., 1972, Ann. Math. Stat., 43, 645
Masiero J., 2017, ApJL, preprint (arXiv:1710.09977)
Matese J., Whitmire D., 1996, ApJ, 472, L41
Matese J. J., Whitman P. G., Whitmire D. P., 1997, Celest. Mech. Dyn. Astron., 69, 77
McNutt R., Zurbuchen T. H., 2016, 41st COSPAR Scientific Assembly, Abstract D1.1-15-16
Meech K. et al., 2017a, MPEC Circ., MPEC 2017-U183
Meech K. J. et al., 2017b, Nature, 552, 378
Oort J. H., 1950, BAN, 11, 91
Rudenko M., 2016, in Chesley S. R., Morbidelli A., Jedicke R., Farnocchia D., eds, IAU Symp. 318: Asteroids: New Observations, New Models. Cambridge Univ. Press, Cambridge, p. 265
Saslaw W. C., Valtonen M. J., Aarseth S. J., 1974, ApJ, 190, 253
Schleicher D. G., 2008, AJ, 136, 2204
Scholz R.-D., 2014, A&A, 561, A113
Stern A., 1987, Icarus, 69, 185
Trilling D. E. et al., 2017, ApJ, 850, L38
Trujillo C. A., Sheppard S. S., 2014, Nature, 507, 471
Tukey J. W., 1977, Exploratory Data Analysis. Addison-Wesley, Reading, MA
Wall J. V., Jenkins C. R., 2012, Practical Statistics for Astronomers. Cambridge Univ. Press, Cambridge
Ye Q.-Z., Zhang Q., Kelley M. S. P., Brown P. G., 2017, ApJ, 851, L5

This paper has been typeset from a TEX/LATEX file prepared by the author.